Modeling the SO_2-Slurry Droplet Reaction

A model of the reaction between SO_2 and calcium-based slurries is presented. The model is coupled with an extensive model of the evaporation process and considers external SO_2 mass transfer and liquid-phase mass transfer of dissolved sulfur and calcium species in both the film surrounding the calcium particles and the bulk liquid phase. The model assumes that particles do not circulate within slurry droplets and that evaporation results in an accumulation of particles at the droplet surface that causes a shift in the controlling mechanisms. Agreement between the model and data available in the literature is excellent.

Gerald H. Newton
John Kramlich
Roy Payne
Energy and Environmental
Research Corporation
Irvine, CA 92718

Introduction

A number of options are currently being considered for reducing SO_2 emissions from existing coal-fired power plants. One of these, duct dry scrubbing, involves the injection of calcium-based slurries into the duct upstream of the ESP. The economics of this process is influenced strongly by sorbent costs. It is, therefore, important to maximize utilization of the calcium hydroxide sorbents to achieve an overall cost-effective process. While there is a general understanding of the mechanisms by which SO_2 is absorbed by slurries, the fundamental processes that limit sorbent utilization have not been identified or quantified with any degree of certainty. A model of the SO_2 absorption process by a slurry droplet was, therefore, developed to provide insight into which of these fundamental processes are rate-limiting.

In the presence of water, SO_2 will react with calcium hydroxide to form calcium sulfite:

$$Ca(OH)_2 + SO_2 = CaSO_3 \cdot \tfrac{1}{2}H_2O + \tfrac{1}{2}H_2O. \qquad (1)$$

Several steps, which occur concurrently with the evaporation of the slurry droplet, are commonly considered, since they are necessary for this reaction to occur:

1. Diffusion of SO_2 from the bulk gas phase to the droplet surface
2. Absorption of SO_2 at the droplet surface
3. Dissolution of SO_2 to form H_2SO_3 and ionization of H_2SO_3 to HSO_3^- and $SO_3^=$
4. Diffusion of these liquid-phase sulfur species inward
5. Dissolution of the $Ca(OH)_2$ particle.

Correspondence concerning this paper should be addressed to G. H. Newton.

The complexity of the above steps makes it difficult to develop a general model that accounts for all of the various processes which in turn may influence the overall rate of SO_2 capture. Initial modeling efforts assumed that only one of the above processes limits the overall rate of SO_2 capture. The one-dimensional model of Jo'zewicz and Rochelle (1984) assumes that the rate of SO_2 capture is controlled by external SO_2 mass transfer. They do, however, offer an argument based on the diffusivity of $Ca(OH)_2$ that the dissolution rate of lime may control the rate of SO_2 capture in some cases. Karlsson and Klingspor (1987) developed two models of the SO_2-slurry droplet reaction: one assumes that external SO_2 mass transfer is controlling, while the second assumes that the dissolution of sorbent is rate-limiting. The first model matched data taken with high slurry concentrations, while the second matched data taken at very low slurry concentrations.

Subsequent modeling efforts contained more detailed descriptions of the process. Damle and Sparks (1986) considered external SO_2 mass transfer, absorption of SO_2 at the droplet surface, dissolution of lime, and a liquid-phase reaction between dissolved SO_2 and sorbent in a slurry droplet. Liquid-phase mass transfer was assumed to be fast, and the slurry droplet was therefore viewed as a well-mixed reactor. The model of Harriott and Kinzey (1986) provides a more detailed description of the interior of a slurry droplet. They assumed that sorbent particles do not circulate within the droplet and that the reaction between dissolved calcium and sulfur species occurs at a spherical front that progresses inward from the droplet surface only after sobent particles at the front have been consumed. Their model assumes that sorbent dissolution is fast and considers both of the external and liquid-phase mass transfer of sulfur species.

The possibility that calcium may dissolve and diffuse out from the center of the droplet has not been considered. Comparison of the concentrations and diffusivities of liquid-phase sulfur and

calcium species reveals that their diffusional rates will be on the same order of magnitude and that the diffusion of calcium outward may be important. The model described here does this.

Model Description

The model makes the following assumptions:

- The liquid-phase ionic reaction between dissolved calcium and sulfur species is instantaneous.
- Water and sorbent particles do not circulate within the droplet.
- Changes in the liquid-phase concentration profiles occur slowly enough so that the pseudosteady-state assumption is valid.
- The heats of reaction and sorbent dissolution are small and can be ignored.
- Thermal gradients within the droplet can be ignored.
- Calcium sulfite is not soluble and precipitates as free standing crystals.
- The droplets and sorbent particles are spherical.

The sulfur capture module described here is coupled with a detailed one-dimensional model of the duct injection process (Cole et al., 1990). The duct injection model considers changes in the volocity of droplets when injected into the duct, droplet temperature, evaporation, gas temperature, gas humidity, and scavenging of particulate matter (ash or sorbent) from the gas phase. The model treats a spray with a distribution of drop sizes.

Ignoring dissolved calcium sulfite is valid once equilibrium has been reached since the solubility of calcium sulfite is approximately two orders of magnitude lower than that of calcium hydroxide. In spray driers, however, calcium sulfite is known to supersaturate by as much as a factor of ten, and in the short times occurring during duct injection it is possible that it could supersaturate by two orders of magnitude. If so, the presence of dissolved sulfite would enhance liquid-phase fluxes during duct injection. Consideration of this is not possible, however, as information on the degree of supersaturation that occurs at short times is not available.

Influence of evaporation

The disposition of sorbent particles during evaporation will influence the rate of internal processes occurring within the slurry droplet. If sorbent particles circulate freely within the droplet, it can be viewed as a mixed reactor where bulk internal diffusional processes are unimportant. If internal circulation were minimal, the diffusion of liquid-phase sulfur species into the droplet would occur over relatively long distances and the overall rate of SO_2 absorption will be slowed.

Work by Constan and Calvert (1963) and by Kinzey (1988) indicate that internal circulation is not significant within slurry droplets. Initially, the sorbent particles are, therefore, viewed as being uniformly distributed throughout the droplet. As water evaporates from the droplet, its surface will recede and encounter particles that were initially near the droplet surface. The receding surface pushes these particles inward and an accumulation of sorbent particles at the droplet surface occurs. This is illustrated in Figure 1. A particle concentration gradient is created between those crowded together at the surface and those within the droplet center that still have the droplet's initial particle concentration. The rate of particle diffusion inward due to this gradient, however, is slow and can be ignored.

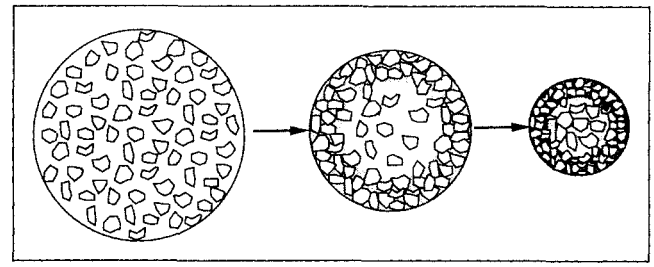

Figure 1. Evaporation causes accumulation of sorbent particles at droplet surface.

Location of reaction fronts

Several researchers (Babu et al., 1984; Chang and Rochelle, 1985; and Sada et al., 1977) found that the rate of the liquid-phase reaction (Eq. 1) is fast compared to the diffusional processes involved. Two types of reaction fronts, local reaction fronts surrounding individual sorbent particles, and a bulk reaction front (illustrated in Figure 2) can, therefore, occur within a slurry droplet if the reaction were assumed to be instantaneous. As the liquid-phase sulfur species diffuse into the droplet, they pass sorbent particles that are simultaneously diffusing calcium outward from their surfaces. A reaction front will develop around each individual sorbent particle when the sulfur species are present in the local bulk liquid phase.

Since the liquid-phase reaction is assumed to be instantaneous, the concentration of sulfur species may drop to zero at some radial position within the slurry droplet. If this occurs, $Ca(OH)_2$ will dissolve at the center of the droplet and diffuse outward to this radial position, and the second type of reaction front shown in Figure 2 will develop.

Sorbent dissolution

Evidence is offered by Moyeda et al. (1988) that the specific surface area of a sorbent may influence the extent of its utilization. The rate an individual sorbent particle dissolves will, therefore, depend on the rate calcium hydroxide molecules leave the sorbent surface and diffuse to the bulk liquid phase where the reaction occurs. The distance that the liquid-phase calcium species must diffuse will be a function of how close the neighboring sorbent particles are. If they were far apart, this

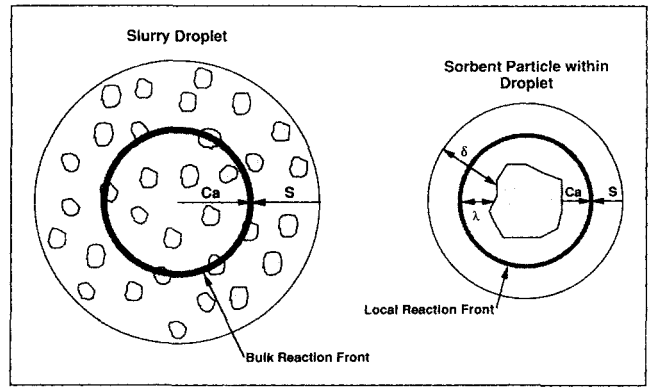

Figure 2. Two types of reaction fronts: one in the bulk liquid phase and the other surrounding individual sorbent particles.

distance would be equivalent to the distance calculated for a particle in an infinite medium (via a Sherwood Number). If the sorbent particles were close, this distance could be calculated as:

$$\delta = \frac{d_p}{2}\left[\frac{1}{(1-w)^{1/3}} - 1\right] \tag{2}$$

When liquid-phase sulfur species are present in the bulk liquid-phase around the sorbent particle, they will also diffuse inward which will decrease the distance liquid-phase calcium must diffuse outward. Calcium will, therefore, diffuse outward to a reaction front that surrounds the sorbent particle while sulfur species diffuse inward. If it is assumed that the pseudosteady-state assumption is valid, the rate of calcium dissolution at the sorbent surface, the rate of calcium hydroxide diffusion outward from the sorbent particle, and the rate of H_2SO_3 and HSO_3- diffusion inward to the sorbent particle can be equated and solved for the reduced film thickness, λ.

The rate of calcium hydroxide dissolution at the particle surface is given by:

$$\text{Dissolution Rate} = \pi d_p^2 \sigma k_d (c_{L,e} - c_L^*). \tag{3}$$

The roughness factor, σ, accounts for the loss in the surface area as the reaction proceeds. Since this factor depends on the unknown structure of a sorbent particle, an empirical factor must be used:

$$\sigma = A/A' = 1 + \exp\left[a(d_p/d_{p,o})^3 - b\right].$$

The assumption that σ equals 2 when 20% of the particle is utilized yields:

$$b = -0.8a$$

where a can be calculated from the initial specific surface area of the sorbent. The rate of calcium hydroxide leaving the particle surface must equal the rate of calcium diffusing anywhere between the particle surface and the reaction front:

$$\pi d_p^2 N_L = 4\pi r^2 D_L \frac{d\hat{c}_L}{dr}.$$

Rearranging and integrating from the particle surface ($\hat{c}_L = c_L^*$) to the reaction front ($\hat{c}_L = 0$ for an instantaneous reaction) yields:

$$\pi d_p^2 N_L = \frac{4\pi D_L c_L^*}{\left(\frac{2}{d_p} - \frac{1}{\lambda + d_p^2}\right)}. \tag{4}$$

The diffusion rate of the liquid-phase sulfur species from the bulk liquid phase (at $d_p/2 + \delta$) is equal to their diffusion rate anywhere between that radial position and the local reaction front (at λ):

$$4\pi(\delta + d_p/2)^2 N_S = 4\pi r^2 \left(D_{HSO_3^-}\frac{d\hat{c}_{HSO_3^-}}{dr} + D_{H_2SO_3}\frac{d\hat{c}_{H_2SO_3}}{dr}\right).$$

Rearranging and integrating from the reaction front ($\hat{c} = 0$ at $d_p/2 + \lambda$) to the outer edge of the ordinary film thickness yields:

$$4\pi(\delta + d_p/2)^2 N_S = \frac{4\pi(D_{HSO_3^-}c_{HSO_3^-} + D_{H_2SO_3}c_{H_2SO_3})}{\frac{1}{(\lambda + d_p/2)} - \frac{1}{(\delta + d_p/2)}}, \tag{5}$$

where $c_{HSO_3^-}$ and $c_{H_2SO_3}$ are the local concentrations in the bulk liquid phase. The term in Eq. 3 and the righthand term in Eq. 4 can be equated and solved for the concentration of calcium hydroxide at the particle surface:

$$c_L^* = \frac{c_{L,e}}{1 + \frac{4D_L}{d_p^2 \sigma k_d\left(\frac{2}{d_p} - \frac{1}{\lambda + d_p}\right)}}. \tag{6}$$

Substituting this into the righthand term of Eq. 4 and equating it to the righthand term in Eq. 5 allow the distance from the particle surface to the local reaction front to be derived:

$$\lambda = \frac{c_{L,e}\delta + \left(\frac{D_{HSO_3^-}c_{HSO_3^-} + D_{H_2SO_3}c_{H_2SO_3}}{\sigma k_d}\right)\left(1 + \frac{2\delta}{d_p}\right)}{c_{L,e} + (D_{HSO_3^-}c_{HSO_3^-} + D_{H_2SO_3}c_{H_2SO_3})\left(1 + \frac{2\delta}{d_p}\right)\left(\frac{1}{D_L} + \frac{2}{d_p\sigma k_d}\right)}. \tag{7}$$

The overall rate of dissolution for a sorbent particle can now be given by:

$$\frac{dn_{Ca}}{dt} = \frac{\pi(c_{L,e} - c_L)}{\frac{1}{d_p^2\sigma k_d} + \frac{\frac{2}{d_p} - \frac{1}{(\lambda + d_p/2)}}{4D_L}}. \tag{8}$$

where c_L equals zero when the liquid-phase sulfur species are present.

Liquid-phase diffusion of sulfur species

The concentration of SO_2 absorbed at the droplet surface is assumed to be at equilibrium and is calculated using Henry's Constant. Once SO_2 is absorbed, it will rapidly react with H_2O to form H_2SO_3, which will subsequently dissociate to HSO_3^- and

$SO_3^=$. The concentration of $SO_3^=$ is negligible and can be ignored. Since both H_2SO_3 and HSO_3^- will diffuse into the droplet interior, both their concentrations must be known. Kinzey (1988) gives the equilibrium concentration of HSO_3^- in terms of the dissociation constant and H_2SO_3:

$$c_{HSO_3^-} = \frac{1}{\sqrt{K_d c_{H_2SO_3}}}. \tag{9}$$

By the pseudosteady-state assumption, the diffusion of H_2SO_3 and HSO_3^- through the bulk phase of the slurry droplet is governed by the partial differential equation:

$$\frac{1}{R^2}\frac{d}{dR}\left(R^2 D_{HSO_3^-}\frac{dc_{HSO_3^-}}{dR} + R^2 D_{H_2SO_3}\frac{dc_{H_2SO_3}}{dR}\right) = \frac{\pi d_p^2 c_{L,e} e_p / w}{\dfrac{1}{d_p^2 \sigma k_d} + \dfrac{\dfrac{2}{d_p} - \dfrac{1}{(\lambda + d_p/2)}}{4D_L}}. \tag{10}$$

where the w term accounts for the reduced liquid volume available for diffusion. Substitution of Eq. 9 allows this equation to be written for $c_{HSO_3^-}$. The first boundary condition of Eq. 10 states that the flux of external mass transfer must equal the flux of liquid-phase sulfur species at the droplet surface. The rate of external mass transfer is calculated from the Sherwood number. Calculation of the Sherwood number accounts for the influence of the high injection velocities that occur when the droplets are injected into the duct. The second boundary condition will depend on the dissolution rate of individual sorbent particles. If it were relatively slow, symmetry requires that:

$$\frac{dc_{HSO_3^-}}{dR} = 0$$

at the center of the drop. If it is fast the concentration of liquid phase sulfur species may drop to zero at some unknown radial location (the location of the bulk reaction front). The flux of dissolved calcium hydroxide outward there must equal the flux of sulfur diffusing inward. The boundary condition at R_{rf}, the bulk reaction front, will be:

$$D_{HSO_3^-}\frac{dc_{HSO_3^-}}{dR} = -D_L\frac{dc_L}{dR}$$

Liquid-phase diffusion of calcium hydroxide

When liquid sulfur species does not penetrate to the center of the droplet, calcium hydroxide will dissolve and diffuse outward. Diffusion of calcium hydroxide will be governed by:

$$\frac{1}{R^2}\frac{d}{dR}\left(R^2 D_L\frac{dc_L}{dR}\right) = \frac{\pi d_p^2 e_p (c_{L,e} - c_L)/w}{\dfrac{1}{d_p^2 \sigma k_d} + \dfrac{\dfrac{2}{d_p} - \dfrac{1}{(\lambda + d_p/2)}}{4D_L}} \tag{11}$$

The boundary conditions of Eq. 11 are:

$$\frac{dc_L}{dR} = 0 \quad @\ R = 0$$

$$c_L = 0 \quad @\ R = R_{rf}.$$

If the conditions within the droplet are such that the reaction front occurs at the droplet surface, the second boundary condition will be that the flux of dissolved calcium hydroxide at the surface equals the rate of external mass transfer with the concentration of SO_2 at the droplet surface equal to zero.

Solution

Three sets of radial shells are utilized in solving these equations. One set monitors the location of sorbent particles within the droplet with the width of these shells set approximately equal to the radius of the sorbent particles. As evaporation begins, the volume of the outer radial shell is decreased, an amount equal to the volume of water evaporated. When the solid volume fraction reaches its maximum allowable value, the volume of the outer radial shell ceases changing and water from the next radial shell inward is removed as evaporation continues. Downs et al. (1980) found evidence that calcium sulfite precipitates as free standing crystals rather than on the surface of the sorbent particles. The volume of solids in a radial shell, therefore, equals the volume of sorbent particles plus the volume of $CaSO_3 \cdot 1/2H_2O$. The volume of calcium sulfite crystals within a radial shell is calculated at each differential time step based on the incremental utilization of sorbent within each radial shell when the liquid-phase sulfur species are present plus the volume of calcium sulfite produced at the bulk reaction front (if located within the radial shell).

Two separate sets of radial shells are used to calculate the concentration profiles of the liquid-phase sulfur and calcium species. The width and number of these shells vary as the location of the bulk reaction front changes. The location of the bulk reaction front within the droplet cannot be calculated *a priori*. The calculation of calcium and sulfur liquid-phase concentration profiles within the droplet, therefore, involves a trial-and-error procedure. Three general cases must be considered:

Case 1.

If the rate of calcium dissolution were relatively slow, sulfur species would penetrate to the center of the droplet and an HSO_3^- concentration would be guessed at the droplet center and the gas-phase SO_2 concentration calculated by a Runge-Kutta routine using Eq. 10 and its outer boundary condition. If the calculated gas-phase SO_2 concentration did not equal the known concentration, the sulfur species concentration at the droplet center is corrected by the secant method and the gas-phase SO_2 concentration recalculated. This is continued until the calculated gas-phase SO_2 concentration is correct.

Case 2.

If the rate of sorbent utilization were relatively fast, the liquid-phase sulfur species concentration would drop to zero at some point within the droplet. The solution approach for this case will be the same as above except that rather than guessing and adjusting the concentration at the droplet center, the radius where the liquid-phase sulfur concentration falls to zero (the reaction front) is guessed. The dissolved calcium hydroxide profile must be calculated first to determine the boundary condition at the reaction front:

- An interative procedure is used where the dissolved calcium hydroxide at the droplet center is guessed, the concentration at

the reaction front calculated by a Runge-Kutta routine using Eq. 11, and, if the concentration at the reaction front did not equal zero, the concentration at the droplet center corrected by the secant method. This is repeated until the concentration of dissolved calcium hydroxide at the reaction front equals zero.

- The gas-phase SO_2 concentration is then calculated using Eq. 10. If the calculated gas-phase SO_2 concentration were incorrect, the radius of the reaction front is corrected by the secant method and the solution procedure (including solving for the calcium profile) repeated. This is continued until the calculated gas-phase SO_2 concentration is correct.

Case 3.

If the rate of sorbent utilization is very fast, the concentration of liquid-phase sulfur species may drop to zero at the droplet surface. The concentration profile of dissolved calcium hydroxide is then solved using the procedure described in case 2 but with the concentration of calcium at the droplet center corrected so that the flux of dissolved calcium hydroxide at the droplet surface equals the rate of external mass transfer with the concentration of SO_2 at the droplet surface set to zero.

At each new differential time step, the model begins by solving for case 1 and, if it could not be solved, by going on to the other two cases. Once the liquid-phase calcium and sulfur concentration profiles have been found, utilization of sorbent particles is calculated from the difference in flux (of sulfur and/or calcium species) into and out of each radial shell. The extent of sorbent utilization is monitored as a function of radial location. This in turn affects the liquid-phase concentration profiles, as the physical properties of the sorbent particles change (the film thickness around the sorbent particles becomes thinner and the roughness factor, σ, becomes smaller as the particle size decreases). The concentration of SO_2 is based on a mass balance with the local concentration determined from the initial SO_2 concentration and the extent of sorbent utilization.

Results and Discussion

Predictions were made with the model to determine the influence of process variables and the controlling subprocesses. The equations used to determine the values of physical parameters are given in Table 1. Although the model includes a term for the dissolution rate at the sorbent surface, no fundamental data taken under typical duct conditions are available that could be used to set their values. The model predictions shown here were made by setting its value so high that it had no influence on model calculations ($c_L^* = c_{L,e}$) . This term was retained in the model, however, as it is possible that dissolution of the sorbent particles surface may be retarded for various reasons. One way this could occur is if the surface of the calcium hydroxide particle reacted with CO_2 to form a layer of relatively insoluble calcium carbonate. The volume fraction of irregularly shaped particles in a packed bed is given by Harriott (1962) as 0.5 to 0.6. The model assumes a 0.6 volume fraction in the layer of sorbent particles that accumulate at the droplet surface. Unless otherwise noted, baseline conditions for the model predictions shown here were: 1,500 ppm SO_2, 20°C approach to saturation, a calcium to sulfur ratio of one, and a 4-μm sorbent particle.

Typical calculated concentration profiles for a 50 droplet, plotted in Figure 3, indicate that rate-controlling processes vary during three stages of a droplet's lifetime. Initially, dissolved $Ca(OH)_2$ diffuses outward from the center of the 50-μm droplet to a (bulk) reaction front within 1 μm of the droplet surface where it meets HSO_3^- (and H_2SO_3) diffusing inward. As the droplet evaporates ($t = 0.5 = 1/2$ droplet lifetime), a layer of sorbent particles accumulates at the droplet surface. The concentration of dissolved $Ca(OH)_2$ increases in this region, the bulk reaction front moves to the droplet surface, and the rate of sulfur absorption approaches the rate of external mass transfer. Near the end of the droplet lifetime ($t = 0.9$), sorbent particles near the droplet surface have been consumed and the bulk reaction front moves inward.

Drop size

Model predictions of the influence of drop size on sorbent utilization are illustrated in Figure 4. As drop size increases, the rate of external mass transfer decreases while the droplet lifetime increases. Above 20 μm, these two factors tend to negate each other and yield the observed weak dependence.

The rate-controlling subprocesses are summarized for a range of drop sizes in Figure 5 by plotting the calculated rate of sulfur absorption divided by the maximum rate of external mass transfer possible. Liquid-phase mass transfer of the sulfur species controls the overall rate at the beginning (before sorbent particles have accumulated at the droplet surface) and at the end (when sorbent at the surface has been consumed) of the lifetime of droplets larger than ~20 μm. External mass transfer is rate-controlling over the intervening portion of their lifetime. Liquid-phase mass transfer of sulfur species also initially controls the overall rate of droplets under 20 μm. Throughout the remainder of their life, the rate of liquid-phase mass transfer (both calcium and sulfur) in the film surrounding the sorbent particles is rate-limiting. (It should be noted that these rate-controlling subprocesses will also vary as other parameters such as slurry concentration or SO_2 concentration change.)

Table 1. Model Parameters

Relationship	Units	Reference
$He = \exp(2.4717 - 2{,}851.1/T_d)$	atm/mol fraction disolved SO_2 (as H_2SO_3)	Rabe and Harris (1963)
$K_d = \exp(22.426 - 1{,}775/T_d - 0.045T_d)$	mol/m^3	Kinzey (1988)
$D_{H_2SO_3} = T_d \exp(-19.895 - 1{,}800/T_d)$	m^2/s	Kinzey (1988)
$D_{HSO_3} = 1.7856 \times 10^{-13} T_d/[1/(4.86T_d - 1{,}100) + 1/(1.46T_d - 390)]$	m^2/s	Kinzey (1988)*
$D_L = 3.954 \times 10^{-9} T_d \exp(-2{,}046/T_d)$	m^2/s	Bird et al. (1960)**

*Accounts for the diffusion of the H^+ ion.
**Derived from the Stokes Einstein equation.

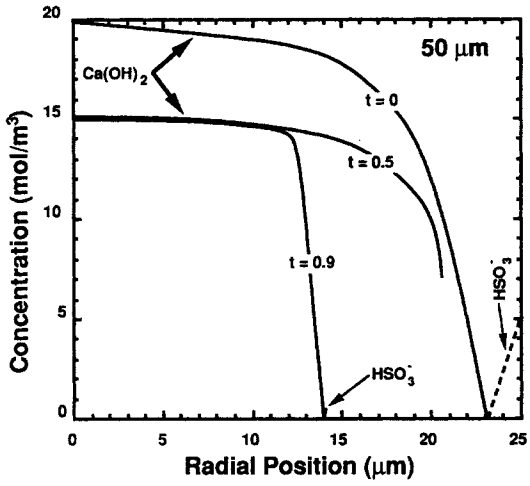

Figure 3. Predicted concentration profiles within a 50-μm droplet at different stages of its lifetime.

——, H_2SO_3; – – –, HSO_3^-; t = time/droplet lifetime

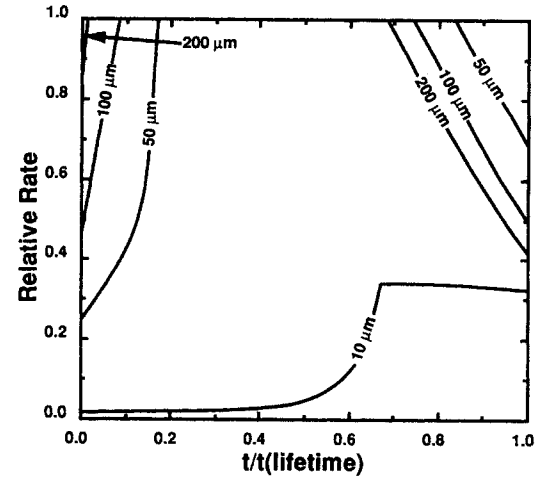

Figure 5. Relative rate of SO_2 absorption over droplet lifetime.

Relative rate is the rate of SO_2 absorption divided by the maximum rate of external SO_2 mass transfer possible.

Stoichiometric ratio

Predicted SO_2 capture as a function of stoichiometric ratio is compared against the data obtained from pilot-scale duct dry scrubbing studies in Figure 6. Agreement between the data and the model is excellent. The size distribution used in these calculations, given in Table 2, was measured for a two-fluid nozzle typical of those used in the duct dry scrubbing process. Capture of SO_2 increases almost linearly up to a stoichiometric ratio of one and levels off at higher ratios. Two factors contribute to this trend. Increasing the stoichiometric ratio is equivalent to increasing the slurry concentration. At stoichiometric ratios above one, increasing the slurry concentration will improve SO_2 capture only during the initial portions of the droplet's life (Figure 5) by increasing the concentration of sorbent particles near the droplet surface and thus reducing the resistance to liquid-phase mass transfer. Throughout the remainder of the droplet's life, the rate of SO_2 capture is limited by either external mass transfer or by liquid-phase mass transfer of sulfur species through a layer of calcium sulfite particles. Increasing the slurry concentration has no effect on these processes.

The second factor which influences the rate of SO_2 capture is the increase in the solids content of the slurry droplets. Increasing the solids content reduces the water content of a drop and increases the number of droplets, which in turn increases the surface area available for both external mass transfer of SO_2 and evaporation. The increased evaporation rate results in a reduced droplet lifetime, which tends to negate the increased rate of external mass transfer.

SO_2 concentration

Literature dealing with the spray drier process (Blythe et al., 1986; Yeh et al., 1985; TVA, 1988) shows sorbent utilization decreasing as SO_2 concentration is increased. Model predictions of the influence of SO_2 concentration, shown in Figure 7, match this trend. Increasing the SO_2 concentration at a constant stoichiometric ratio increases the slurry concentration, which

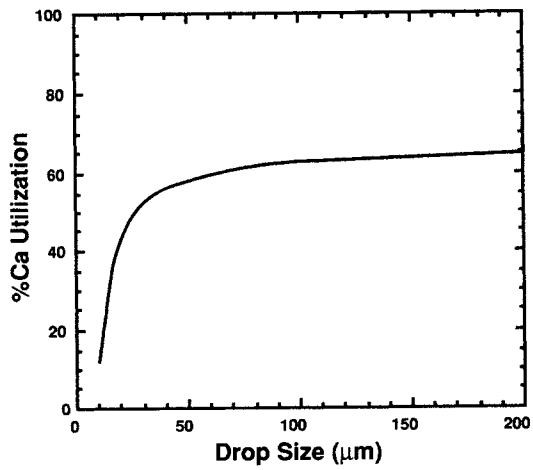

Figure 4. Predicted influence of drop size on utilization.

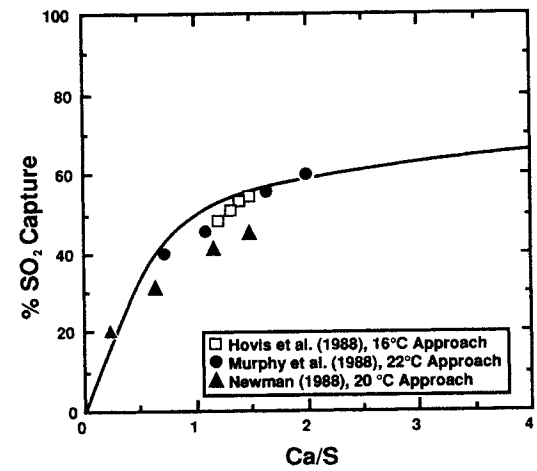

Figure 6. Model predictions vs. data from pilot-scale duct dry scrubbing studies.

Solid symbols taken from regression formula.

Table 2. Typical Spray Size Distribution

Drop (μm)	Weight Fraction
16.6	0.277
33.6	0.565
63.1	0.158

has similar effects on the process as increasing the stoichiometric ratio: the increasing solids content of the droplets results in a decrease in the droplet lifetime. The decrease in droplet lifetime is the primary cause of the decrease in SO_2 capture, as SO_2 concentration is increased.

Approach to saturation

The agreement between the data taken from literature on the pilot-scale duct dry scrubbing studies and model predictions, illustrated in Figure 8, is excellent. The primary cause of the trends observed in Figure 8 is the increase in droplet lifetime as the approach to saturation is decreased. A secondary factor that contributes to these trends is the increase in the quantity of spray as the approach to saturation is reduced. This increase in the quantity of spray increases the surface area available for external mass transfer and decreases the slurry concentration, both of which tend to increase utilization.

Summary

A model of the reaction between SO_2 and slurry droplets was presented. The model considers the internal liquid-phase mass transfer of dissolved sulfur and calcium species in both the film surrounding the sorbent particles and in the bulk liquid phase. A key assumption of the model is that particles do not circulate within the slurry droplets. Sorbent particles, therefore, accumulate at the receding surface of an evaporating slurry droplet. This results in a shift in the rate-controlling mechanism.

The model indicates that the rate-limiting processes in droplets larger than ~20 μm (under typical duct conditions) vary during the three stages of the droplet evaporation:

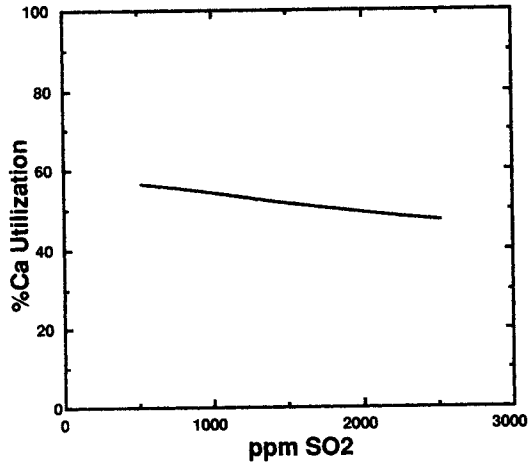

Figure 7. Predicted influence of SO_2 concentration on utilization.

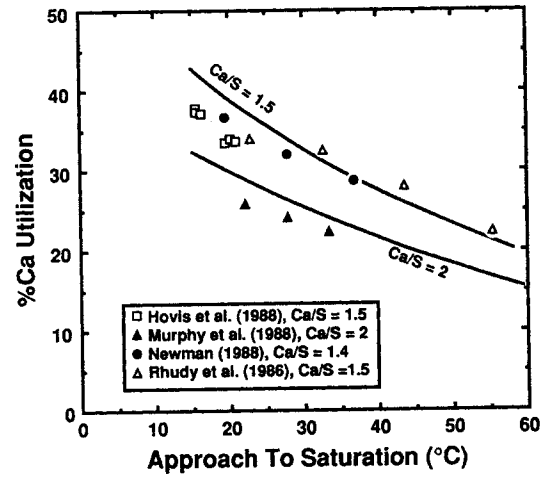

Figure 8. Model predictions vs. data from pilot-scale duct dry scrubbing studies.
Solid symbols taken from regression formula.

- Initially liquid-phase diffusion of sulfur species is rate-limiting.
- External mass transfer is rate-limiting, as evaporation results in an accumulation of sorbent particles at the droplet surface.
- Liquid-phase mass transfer becomes important at the end of a droplet's lifetime as sorbent particles at the droplet surface are consumed.

Rate-limiting subprocesses vary in two stages in droplets smaller than ~20 μm:

- Initially liquid-phase diffusion of sulfur species is rate-limiting.
- Liquid-phase diffusion in the film surrounding individual sorbent particles limits during the remaining portion of the droplet's lifetime.

The model was compared to data from the spray drier literature and the duct dry scrubber literature. The model reproduced trends from the spray drier literature, and agreement between the model and the data from the duct dry scrubber literature was excellent.

Acknowledgment

This work was supported by the U.S. Department of Energy, Pittsburgh Energy Technology Center, under contract DE-AC22-88PC88873. The authors are grateful to Prof. Peter Harriott of Cornell University for his advice and comments during the development of this work.

Notation

A = surface area of sorbent, m^2
A_s = surface area of a spherical sorbent particle with no porosity, m^2
c = concentration in bulk liquid phase, mol/m^3
c_L^* = concentration of calcium hydroxide at particle surface, mol/m^3
$\hat{c}$ = local concentration of diffusing species in films around particle, mol/m^3
d_p = sorbent particle diameter, m
D = liquid-phase diffusivity, m^2/s
He = Henry's Constant, atm/mole fraction
k_d = dissolution rate constant at particle surface, m/s
K_d = dissociation constant of H_2SO_3, mol/m^3
n = moles
N = flux, $mol/m^2 \cdot s$

R = radial position within droplet, m
t = time, s
T = temperature, K
w = volume fraction water in a drop

Greek letters

λ = film thickness when diffusion of liquid-phase sulfur species to particle is considered, m
δ = film thickness around a sorbent particle, m
μ = viscosity, g/m · s
σ = roughness factor

Subscripts

d = drop
e = equilibrium
L = calcium hydroxide
o = initial
p = particle
rf = reaction front

Literature Cited

Babu, D. R., G. Narsimhan, and C. R. Phillips, "Absorption of Sulfur Dioxide in Calcium Hydroxide Solutions," *Ind. Eng. Chem. Fund.*, **23,** 370 (1984).

Bird, R. B., W. E. Stewart, and E. N. Lightfoot, *Transport Phenomena,* Wiley, New York (1960).

Blythe, B. M., R. Smith, M. McElroy, R. Rhudy, V. Bland, and C. Martin, "EPRI Pilot Testing of SO_2 Removal by Calcium Injection Upstream of a Particulate Control Device," *Proc. Symp. on Dry SO_2/NO_x Control Tech.*, EPRI CS-4966, Raleigh, NC (1986).

Chang, C. S., and G. T. Rochelle, "SO_2 Absorption into NaOH and Na_2SO_3 Aqueous Solutions," *Ind. Eng. Chem. Fund.*, **24,** 7 (1985).

Cole, J. C., G. H. Newton, J. C., Kramlich, and R. Payne, "Global Evaluation of Mass Transfer Effects: In-Duct Flue Gas Desulfurization," Final Report U.S. DOE, PETC Contract DE-AC22-88PC88873 (1990).

Constan, G. L., and S. Calvert, "Mass Transfer in Drops under Conditions That Promote Oscillation and Internal Circulation," *AIChE J.*, **9,** 109 (1963).

Damle, A. S., and L. E. Sparks, "Modeling of SO_2 Removal in Spray-Dryer Flue-Gas Desulfurization System," *Proc. AIChE Meeting,* New Orleans (1986).

Downs, W., W. J. Sanders, and C. E. Miller, "Control of SO_2 Emissions by Dry Scrubbing," *Proc. Amer. Power Conf.*, **42,** 262 (1980).

Harriott, P., "Mass Transfer to Particles: I. Suspended in Agitated Tanks," *AIChE J.*, **8,** 93 (1962).

Harriott, P., and M. Kinzey, "Modeling the Gas and Liquid-Phase Resistances in the Dry Scrubbing Process for SO_2 Removal," *Proc.* Pittsburgh *Coal Conf.* (1986).

Hovis, L. S., R. E. Valentine, B. J. Jankura, P. Chu, and J. C. S. Chang, "E-SO_x Pilot Evaluations," *Proc. Comb. FGD and Dry SO_2 Control Symp.*, St. Louis (1988).

Jo'zewicz, W. and G. Rochelle, "Modeling of SO_2 Removal by Spray Dryers," *Proc.* Pittsburgh *Coal Conf.* (1984).

Karlsson, H. T., and J. Klingspor, "Tentative Modeling of Spray-Dry Scrubbing of SO_2," *Chem. Eng. Tech.*, **10,** 104 (1987).

Kinzey, M., "Modeling the Gas and Liquid-Phase Resistances in the Dry Scrubbing Process for Sulfur Dioxide Removal," Masters Thesis, Cornell Univ. (1988).

Moyeda, D. K., G. H. Newton, J. F. La Fond, R. Payne, and J. C. Kramlich, "Rate-Controlling Processes and Enhancement Strategies in Humidification for Duct SO_2 Capture," EPA/600/S2-88/047, U.S. EPA, NTIS No. PB 88-245915/AS (1988).

Murphy, K. R., E. A. Samuel, and A. Demian, "In-Duct Scrubbing (IDS) Process," *Proc. Comb. FGD and Dry SO_2 Control Symp.*, St. Louis (1988).

Newman, J. T., "Confined Zone Dispersion (CZD) Process," *Proc. Comb. FGD and Dry SO_2 Control Symp.*, St. Louis (1988).

Rabe, A. E., and J. F. Harris, "Vapor Liquid Equilibrium Data for the Binary System, Sulfur Dioxide and Water," *J. of Chem. Eng. Data.*, **8,** 333 (1963).

Rhudy, R., M. McElroy, and G. Offen, "Status of Calcium-Based Dry Sorbent Injection SO_2 Control," *Symp. of Flue Gas Desulf.*, Atlanta (1986).

Sada, E., H. Kumazawa, and M. A. Butt, "Single Gas Absorption with Reaction in a Slurry Containing Fine Particles," *Chem. Eng. Sci.*, **32,** 1165 (1977).

Tennessee Valley Authority, "10-MW Spray Dryer/ESP Pilot-Plant Test Program High-Sulfur Coal Test Phase (Phase III)." Final Report TVA/OP/ED&T-88/35 (1988).

Yeh, J. T., R. J. Demski, and J. I. Joubert, "Performance of a Spray Dryer/ESP Flue Gas Cleanup System During Testing at the Pittsburgh Energy Technology Center," *EPA/EPRI Symp. on Flue Gas Desulf.*, Cincinnati (1985).

Manuscript received Feb. 28, 1990, and revision received Oct. 11, 1990.